FLOW IN SPIRAL CHANNELS OF SMALL CURVATURE AND TORSION

Y.M. Stokes

Department of Applied Mathematics, The University of Adelaide, Australia

Abstract We compute the flow in an open helical (or spiral) channel and must, as part of the solution process, find the free surface shape which is dependent on geometrical and flow parameters. We extend work on closed spiral flows to open spiral flows, seeking for helically symmetric solutions as a first step towards solving what could be a full three-dimensional problem. For completely general channel geometries numerical methods must be used. A particular difficulty is determining the points of contact of the free surface with the channel walls. We consider channels of small curvature, small torsion and semicircular cross-section and compare with an analytic solution obtainable under these conditions.

Keywords: helical-channel flow, free surface

1. INTRODUCTION

Considerable literature exists concerning mathematical modelling of fully developed flow in *closed* helically-coiled pipes. See, for example, the review given by Germano (1989) and the recent papers of Zabielski and Mestel (1998a,1998b). These studies have been motivated by a desire to better understand flows in curved geometries such as arise in many piping systems, and the human blood circulation system in particular. They have shown that, for this type of flow, a steady-state solution can be computed, comprising a velocity component along the axis of the pipe and a secondary cross flow.

By comparison, flows in *open* helical channels (see Figure 1), which differ most significantly from their closed-pipe counterparts in having a free surface, have received little attention. Yet, these flows too are of practical importance. They occur in spiral particle separators used in the mining and mineral-processing industries and, indeed, a better understanding of the flow would be of considerable benefit to the design of such equipment. They are also of relevance to helical-coil distillation columns used in fractionation of petroleum products (Morton *et*

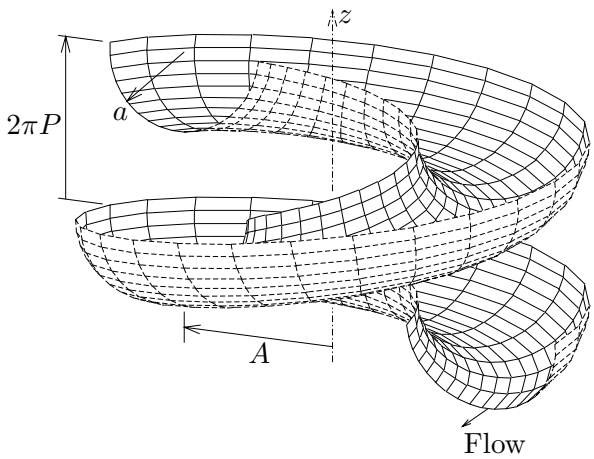

Figure 1 A helical channel of semi-circular cross-section.

al. 1964) and other curved piping systems that run only partly full. Some 3D simulation of flows in spiral particle separators, using volume-of-fluid methods and the commercial CFD program FLUENT, has been done recently by Matthews *et al.* (1996,1997) and these papers also include discussion of other work that relates specifically to flow in spiral separators. However, there is a need for a more basic analysis of helical-channel flows, including parameter studies, and we here begin to address this.

We proceed in a similar manner to the studies of closed coiled pipes by Germano and others, in first finding a steady-state solution that is also independent of axial position. This permits a two-dimensional analysis in the cross-section plane. As part of the solution process, we must determine the free-surface profile of the fluid in the channel, making this analysis significantly different from and more complex than fully developed flows in closed pipes. It is obvious that the shape of the free surface will be primarily determined by the curvature of the helix and the flow rate, so that, at this stage, we ignore surface tension.

2. THE EQUATIONS

We consider a right-hand helical channel of semi-circular cross-section as shown in Figure 1, with gravity acting in the $-z$ direction. The helix has radius A and pitch $2\pi P$; the channel has radius a.

Previous work on flows in closed helical pipes has given considerable attention to the derivation of orthogonal coordinate systems for helically symmetric flows; see, for example, Germano (1982) and Zabielski &

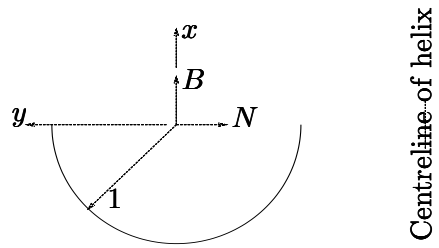

Figure 2 Cross section of channel showing coordinates.

Mestel (1998a). Since we are considering channels of small curvature (certainly with $A > a$) the system of Germano (1982) is suitable and we adopt this. For helical pipes of strong curvature, i.e. $a > A$, the system described by Zabielski and Mestel (1998a) should be used, which under conditions of small curvature is equivalent to the system of Germano.

The dimensionless continuity and steady Navier-Stokes equations for a helically-symmetric pressure-driven flow are given in Germano (1989). We modify these, substituting driving terms due to gravity for the axial pressure gradient term. As in Germano (1989) we assume that the dimensionless curvature ϵ is small and drop terms of order ϵ and higher. We further simplify the equations by restricting our attention to flows for which $\lambda/\mathcal{R}$ is small, also of order ϵ — equivalent to an assumption of small torsion. Here, $\lambda = P/A$ is the ratio of torsion to curvature and $\mathcal{R} = Ua/\nu$ is the Reynolds number for the flow with characteristic velocity U and kinematic viscosity ν. Then, for a flow driven by gravitational acceleration g and using the coordinate system shown in Figure 2 with lengths normalised to give a channel radius of 1, the equations become

$$\frac{\partial v}{\partial x} + \frac{\partial w}{\partial y} = 0, \tag{1.1}$$

$$v\frac{\partial u}{\partial x} + w\frac{\partial u}{\partial y} = \nabla^2 u - \frac{\lambda\mathcal{R}}{\mathcal{F}^2\sqrt{1+\lambda^2}}, \tag{1.2}$$

$$v\frac{\partial v}{\partial x} + w\frac{\partial v}{\partial y} = -\frac{\partial p}{\partial x} + \nabla^2 v - \frac{\mathcal{R}^2}{\mathcal{F}^2\sqrt{1+\lambda^2}}, \tag{1.3}$$

$$v\frac{\partial w}{\partial x} + w\frac{\partial w}{\partial y} - \frac{1}{2}Ku^2 = -\frac{\partial p}{\partial y} + \nabla^2 w, \tag{1.4}$$

where u is the axial flow velocity, v and w are the secondary flow velocity components in the x and y directions respectively, p is the pressure, $\mathcal{F} = U/\sqrt{ag}$ is the Froude number and $K = 2\epsilon\mathcal{R}^2$ is the Dean number associated with the centrifugal force acting on the flow.

The boundary conditions on the channel wall are simply the no-slip conditions

$$u = v = w = 0. \tag{1.5}$$

On the free surface $F(x, y) = 0$ having normal $(0, n^x, n^y)$ we have (ignoring surface tension) the zero-stress conditions (Batchelor 1967)

$$n^x \frac{\partial u}{\partial x} + n^y \frac{\partial u}{\partial y} = 0, \tag{1.6}$$

$$-pn^x + 2n^x \frac{\partial v}{\partial x} + n^y \left(\frac{\partial w}{\partial x} + \frac{\partial v}{\partial y} \right) = 0, \tag{1.7}$$

$$-pn^y + n^x \left(\frac{\partial w}{\partial x} + \frac{\partial v}{\partial y} \right) + 2n^y \frac{\partial w}{\partial y} = 0, \tag{1.8}$$

and the kinematic condition

$$v \frac{\partial F}{\partial x} + w \frac{\partial F}{\partial y} = 0 \quad \text{or, equivalently,} \quad vn^x + wn^y = 0. \tag{1.9}$$

The system (1.1)–(1.4) must be solved subject to boundary conditions (1.5)–(1.9) for the velocity and pressure distributions in the flow domain as well as the free-surface shape $F(x, y) = 0$.

3. AN ANALYTIC SOLUTION

For some choices of the flow parameters, the secondary flow will be small and it is reasonable to drop the inertial terms from the equations. Then (1.2)–(1.4) simplify to:

$$0 = \nabla^2 u - \frac{\lambda \mathcal{R}}{\mathcal{F}^2 \sqrt{1 + \lambda^2}}, \tag{1.10}$$

$$0 = -\frac{\partial p}{\partial x} + \nabla^2 v - \frac{\mathcal{R}^2}{\mathcal{F}^2 \sqrt{1 + \lambda^2}}, \tag{1.11}$$

$$-\frac{1}{2} K u^2 = -\frac{\partial p}{\partial y} + \nabla^2 w. \tag{1.12}$$

Also, with small secondary flow the free surface will be close to flat and we may find an approximate analytic solution to (1.10)–(1.12) which satisfies the free-surface boundary conditions at $x = 0$. Tuck (1998) has shown that under these circumstances, the free surface is given by the quintic polynomial expression

$$x = \left[\frac{K}{768} \frac{\lambda^2}{\mathcal{F}^2 \sqrt{1 + \lambda^2}} \right] y \left(15 - 8y^2 + 3y^4 \right). \tag{1.13}$$

4. A NUMERICAL SOLUTION METHOD

The more general problem specified in Section 2 above must be solved numerically and, to this end, we have implemented the following iterative algorithm in the finite-element PDE solver *Fastflo*[1]:

- Assume some initial flow domain, in particular a free surface shape. Define a finite-element mesh, consisting of nodes connected by elements, over this domain.
- Loop

  1: Find the velocity and pressure distribution in this domain by solving (1.1)–(1.4) subject to boundary conditions (1.5)–(1.8). The kinematic condition (1.9) may not be satisfied.

  2: Compute $Q = \int_F (vn^x + wn^y)^2 ds$ over the free surface. Q is a measure of flux through the free surface which is zero when the free-surface shape has been determined correctly and the kinematic condition (1.9) is satisfied.

  3: If Q is less than some tolerance then exit the loop — the problem is solved. Otherwise continue to Step 4

  4: Compute the displacement of each mesh node in the flow domain in a small pseudo-time step Δt: $(\Delta x, \Delta y) = (v, w)\Delta t$. Move each node to obtain a new flow domain and return to Step 4.

Because the flow equations are non-linear, Step 4 of the above loop itself requires an iterative procedure. We linearise the equations and use an augmented Lagrangian formulation which yields the following system:

$$v_{n-1}\frac{\partial u_n}{\partial x} + w_{n-1}\frac{\partial u_n}{\partial y} = \nabla^2 u_n - \frac{\lambda \mathcal{R}}{\mathcal{F}^2\sqrt{1+\lambda^2}}, \tag{1.14}$$

$$\begin{aligned} v_{n-1}\frac{\partial v_n}{\partial x} + w_{n-1}\frac{\partial v_n}{\partial y} &= \\ -\frac{\partial}{\partial x}\left[p_{n-1} - \beta\left(\frac{\partial v_n}{\partial x} + \frac{\partial w_n}{\partial y}\right)\right] &+ \nabla^2 v_n - \frac{\mathcal{R}^2}{\mathcal{F}^2\sqrt{1+\lambda^2}}, \end{aligned} \tag{1.15}$$

$$\begin{aligned} v_{n-1}\frac{\partial w_n}{\partial x} + w_{n-1}\frac{\partial w_n}{\partial y} - \frac{1}{2}Ku_n^2 &= \\ -\frac{\partial}{\partial y}\left[p_{n-1} - \beta\left(\frac{\partial v_n}{\partial x} + \frac{\partial w_n}{\partial y}\right)\right] &+ \nabla^2 w_n, \end{aligned} \tag{1.16}$$

[1]Developed by CSIRO, Australia

$$p_n = p_{n-1} - \beta \left(\frac{\partial v_n}{\partial x} + \frac{\partial w_n}{\partial y} \right). \tag{1.17}$$

Note that (1.17) has been substituted for p_n in (1.15) and (1.16) and replaces the continuity condition (1.1) which is satisfied when $p_n = p_{n-1}$; β is an arbitrary constant chosen to speed convergence. Now Step 4 above expands to

1: Set $n = 0$. Initialise $u_0 = v_0 = w_0 = p_0 = 0$ if necessary. Execute the following loop until the pressure field has converged.

   (a) $n = n + 1$

   (b) Solve (1.14) for the axial velocity u_n subject to boundary condition (1.6).

   (c) Solve (1.15) and (1.16) as a coupled system subject to boundary conditions (1.7) and (1.8) for v_n and w_n.

   (d) Use (1.17) to update the pressure field p_n.

5. COMPARISON OF NUMERICAL AND ANALYTIC SOLUTIONS

It is of interest to compare numerical results with the analytic solution. For flows having a free surface that is only slightly perturbed from flat the two methods compare well excepting at the end points. This is seen from a comparison of curves (a) and (b) in Figure 3. Curve (a) is the analytic result (1.13) and curve (b) is the free surface shape obtained by the numerical method of Section 4 starting with a flat free surface. The parameters for this flow were

$$K = 2, \quad G = \frac{\lambda \mathcal{R}}{\mathcal{F}^2 \sqrt{1+\lambda^2}} = 2, \quad G\frac{\mathcal{R}}{\lambda} = \frac{\mathcal{R}^2}{\mathcal{F}^2 \sqrt{1+\lambda^2}} = 20$$

chosen such that the free surface is close to flat. Locally near the points of attachment of the free surface to the channel wall the two solutions do not agree, because the numerical solution scheme pins the free surface to the channel wall at the points of attachment initially assumed. If we use (1.13) to estimate the points of attachment, then the numerical and analytic solutions for this set of parameters agree extremely well over the whole of the free surface, as shown by curve (c) in Figure 3 which is virtually identical to the analytic solution curve (a).

As the flow parameters are changed to give a flow with a larger cross-flow component and a free surface that is more greatly perturbed from flat, the agreement between the numerical and analytic solutions reduces, as for example in Figure 4. This is to be expected since the greater

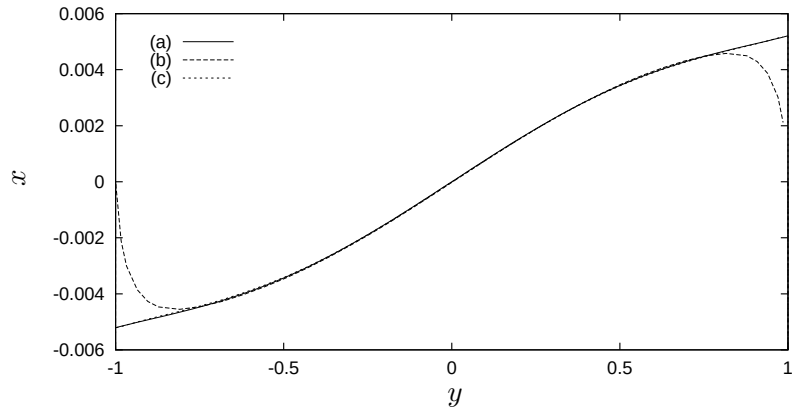

Figure 3 Free surface shape for a flow with $K = 2$, $G = 2$, $G\mathcal{R}/\lambda = 20$. (a) Analytic solution (1.13), (b) numerical solution starting with a flat free surface and (c) numerical solution starting with a straight line free surface between the attachment points indicated by (1.13), almost indistinguishable from (a).

the perturbation, the less applicable is the analytic solution. However, in this parameter regime, the accuracy of the numerical solution, at least near the end points of the free surface, is significantly affected by inaccurate location of the points of attachment of the free surface to the channel wall.

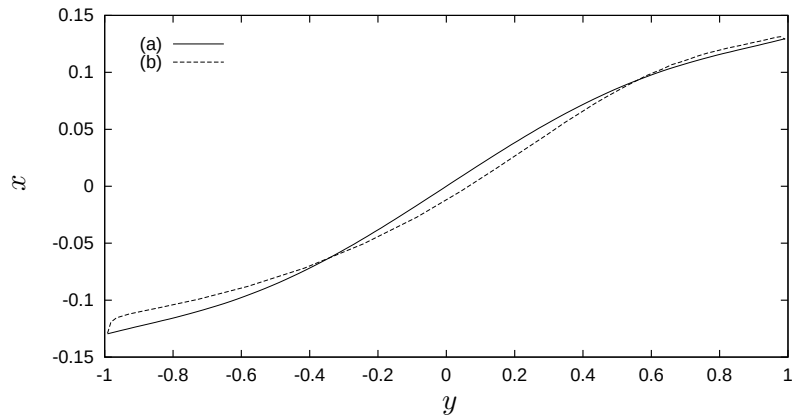

Figure 4 Free surface shape for a flow with $K = 5$, $G = 20$, $G\mathcal{R}/\lambda = 200$. (a) Analytic solution (1.13), (b) numerical solution starting with a straight line free surface between the attachment points indicated by (1.13).

6. CONCLUSION

We have developed a numerical code for computing flows in helical channels of small curvature and torsion. This compares well with the analytic solution obtained for flows having a free surface only slightly perturbed from flat. However, the current numerical scheme requires that we *a priori* locate the points of attachment of the free surface to the channel wall and these points then do not change. Guessing these points to sufficient accuracy for flows with large free-surface perturbation is extremely difficult. Further work is underway to develop a numerical method that finds the free-surface shape, including the points of attachment to the channel wall, as part of the solution procedure.

Acknowledgments

This work was funded by a 1998 Australian Research Council (ARC) Small Grant to J.P. Denier, J.A.K. Stott and E.O. Tuck, and continued into early 1999 with additional funding from E.O. Tuck. Present support is by way of an ARC Postdoctoral Fellowship to the author. All support is gratefully acknowledged, as is discussion with those mentioned above.

References

G.K. Batchelor (1967), *An Introduction to Fluid Dynamics*. Cambridge University Press, Appendix 2.

M. Germano (1982), On the effect of torsion on a helical pipe flow. *J. Fluid Mech.* 125, 1–8.

M. Germano (1989), The Dean equations extended to a helical pipe flow. *J. Fluid Mech.* 203, 289–305.

B.W. Matthews, C.A.J. Fletcher, A.C. Partridge, and T. Jancar (1996), Computational simulation of spiral concentrator flows in the mineral processing industry. *Chemeca '96*.

B.W. Matthews, C.A.J. Fletcher, and A.C. Partridge (1997), Computational simulation of fluid and dilute particulate flows on spiral concentrators. *Inter. Conf. on CFD in Mineral & Metal Processing and Power Generation*, CSIRO, 1997, 101–109.

F. Morton, P.J. King, and A. McLaughlin (1964), Helical-coil distillation columns Part I: Efficiency studies. *Trans. Instn Chem. Engrs* 42, T285–T295.

E.O. Tuck (1998), Personal communications.

L. Zabielski and A.J. Mestel (1998a), Steady flow in a helically symmetric pipe. *J. Fluid Mech.* 370, 297–320.

L. Zabielski and A.J. Mestel (1998b), Unsteady blood flow in a helically symmetric pipe. *J. Fluid Mech.* 370, 321–345.